Eigenmode Distortion Analysis for Motion Cueing Evaluation in Fixed-Wing Aircraft Simulators

Stoev, Stanimir; van Paassen, Rene; Stroosma, Olaf; Miletovic, Ivan; Mulder, Max

DOI
10.2514/6.2019-0179

Publication date
2019

Document Version
Final published version

Published in
AIAA Scitech 2019 Forum

AIAA SciTech Forum
7-11 January 2019, San Diego, California
AIAA Scitech 2019 Forum

10.2514/6.2019-0179

Eigenmode Distortion Analysis for Motion Cueing Evaluation in Fixed-Wing Aircraft Simulators

S. Stoev*, M. M. van Paassen†, O. Stroosma‡, I. Miletović§, and M. Mulder¶

The Eigenmode Distortion (EMD) analysis is a novel method for objective evaluation of simulator motion cueing fidelity, developed at Delft University of Technology. It expresses the distortions of the perceived motion cues in terms of the dynamic modes of a linear model of the vehicle and has been applied to assess rotorcraft simulations. This paper presents the adaptation of EMD for fixed wing aircraft, including performing the analysis at the pilot station instead of the centre of gravity. The method is applied to a combined linear model of a Cessna Citation 500 aircraft and the Classical Washout Algorithm (CWA). EMD is compared to the current state-of-the-art objective method, the Objective Motion Cueing Test (OMCT), which does not consider the dynamics of the simulated vehicle in its analysis. The two methods show different results in their cueing fidelity assessment of four CWA configurations. An experiment with six pilots is performed in the SIMONA Research Simulator to test the capability of EMD and OMCT to predict the cueing fidelity as perceived by pilots. The subjects perform pairwise comparisons between the four CWA configurations by exciting the short period dynamics of the aircraft. Results indicate that preferences vary considerably between pilots, causing both EMD and OMCT to show poor, but similar, predictive capabilities.

I. Introduction

The motion cues provided by ground-based flight simulators can usually not fully match the cues present in the real vehicle. Motion Cueing Algorithms (MCAs) are employed to translate the cues calculated by the simulator's vehicle model into simulator motions that fit inside the simulator's motion space. In this process the cues are inevitably distorted, which might decrease the simulator's usefulness in representing reality for the pilot.

The design and tuning of the MCA must reconcile the two competing goals of providing realistic cues and limiting the simulator motion. The most widely used procedure for this process relies heavily on subjective evaluations by experienced pilots [1]. The relative lack of objective metrics to characterize "good" motion can lead to vastly different motion profiles between operational simulators.[2].

The undesirability of a purely subjective evaluation of motion cueing quality was already recognized in the 1970s, when Sinacori [3] proposed a simple gain and phase distortion test of the MCA at a frequency of 1 rad/s, together with boundaries for low, medium, and high fidelity. This was later refined and expanded into tuning procedures based on this test by Schroeder[4] and Gouverneur[5].

Since then further research [6–8] has resulted in the current state-of-the art objective evaluation method: the Objective Motion Cueing Test (OMCT) [9], which is now part of the latest ICAO criteria for qualification of flight simulation training devices [10]. In OMCT, a frequency response analysis of the MCA and motion hardware dynamics is performed for all six axes of motion in twelve frequency points between 0.1 rad/s to 15.97 rad/s thus giving a more complete representation of the motion system's charateristics than the Sinacori test at 1 rad/s.

*MSc Student,Control and Simulation section, Faculty of Aerospace Engineering, P.O. Box 5058, 2600GB Delft, The Netherlands;s.stoev@student.tudelft.nl

†Associate Professor, Control and Simulation section, Faculty of Aerospace Engineering, P.O. Box 5058, 2600GB Delft, The Netherlands; m.m.vanpaassen@tudelft.nl

‡Researcher,Control and Simulation section, Faculty of Aerospace Engineering, P.O. Box 5058, 2600GB Delft, The Netherlands; o.stroosma@tudelft.nl. Senior Member AIAA

§PhD Student,Control and Simulation section, Faculty of Aerospace Engineering, P.O. Box 5058, 2600GB Delft, The Netherlands; i.miletovic@tudelft.nl

¶Professor, Control and Simulation Section, Faculty of Aerospace Engineering, P.O. Box 5058, 2600GB Delft, The Netherlands;m.mulder@tudelft.nl. Associate Fellow, AIAA.

However, at the time of writing, fidelity regions comparable to the ones proposed by Sinacori and Schroeder are based on the averaged response of ten simulators of various qualification levels and simulated aircraft types [9]. Alternative fidelity criteria based on pilot task performance during flight tasks are investigated [1]. Despite that no definitive fidelity criteria have yet been identified, OMCT has also been used for tuning of the MCA. An example is the study by De Ridder and Roza [11], where OMCT is used in an automatic optimization process of MCA parameters.

One drawback shared between the method of Sinacori and OMCT is that both tests only evaluate the MCA itself, and in the case of OMCT, the combination with the motion hardware dynamics. The simulated vehicle dynamics are not included in either test, and it is assumed that the MCA response to motion cues provided by the vehicle model is sufficiently similar to the combined responses of the individual motion axis responses tested in the Sinacori test or OMCT. Recent work by Dalmeijer et al.[12] indicates that cross-couplings and other non-linearities in the MCA might interact with vehicle dynamics to further amplify or attenuate certain cues at certain frequencies in ways that are not apparent in an OMCT evaluation. In order to further study this problem, a new objective method for motion cueing fidelity analysis, named Eigenmode Distortion (EMD), is developed by Miletović et al. [13]. EMD evaluates the distortions of the perceived motion cues imposed by the MCA while taking the dynamics of the simulated vehicle into account. This is made possible by coupling the dynamics of the MCA and the vehicle into a single combined system, enabling the representation of the human perceived motion cues in terms of the *dynamic modes* of the vehicle. Originally EMD was developed for and applied in rotorcraft simulation [13].

The purpose of this study is to investigate the use of EMD in fixed-wing aircraft simulations. To this end EMD is applied to a linear model of a Cessna Citation 500 for symmetric flight and the Classical Washout Algorithm (CWA) [14] used as the MCA. In addition, EMD is compared to OMCT for four CWA configurations. The capability of both methods to predict the cueing fidelity as perceived by pilots is tested in a piloted experiment in the SIMONA Research Simulator (SRS) [15] at the Delft University of Technology.

This paper is structured as follows. The general principles of EMD and its adaptation for use in fixed-wing aircraft is examined in Section II, followed by the practical application of EMD and comparison to OMCT in Section III. Next, the experiment to evaluate EMD's capabilities is discussed in Section IV with the results being shown in Section V. The paper ends with a discussion in Section VI and in Section VII the conclusions are given.

II. EMD application in fixed-wing aircraft

A. Main principles of the methodology

The current state-of-the-art method for objective evaluation of the motion cueing fidelity − the Objective Motion Cueing Test (OMCT) − analyses the frequency response of the Motion Cueing System (MCS) to a set of sine-wave input signals for the human perceived motion cues − specific forces and angular rates along all six simulator axes. The same input signals are used irrespective of the aircraft type being simulated. While OMCT gives a very detailed picture on the combined performance of the Motion Cueing Algorithm (MCA) and the motion hardware dynamics, its input signals do not realistically represent motions experienced during simulations of different aircraft types [16]. In addition, the response to each signal is studied in isolation, while the motions of the aircraft, and consequently the cues sent to the MCA, are linked through the vehicle dynamics.

The Eigenmode Distortion (EMD) analysis aims to address these shortcomings. It approaches the evaluation of the motion cueing fidelity from a different perspective. While OMCT analysis is performed in the frequency domain, EMD investigates the distortion of the motion cues imposed by the MCA in terms of eigenvectors representing the dynamic modes of the simulated vehicle. In this paper a typical fixed-wing aircraft will be considered. In the EMD analysis, linear dynamic models for the aircraft and MCA are used. They are presented respectively in Eq. (1) for symmetric flight and Eq. (2) for longitudinal motions. Here the p superscript refers to the dynamics experienced by the pilot and the m superscript to the MCA dynamics. The δ notation indicates that the states and inputs are in fact perturbations relative to the initial condition. Furthermore, while on the one hand the aircraft state vector $\delta_{\vec{x}}^{p}$ is known from classical flight dynamics, the exact formulation of $\delta_{\vec{x}}^{m}$ depends on the used MCA. On the other hand, the MCA inputs $\delta_{\vec{u}}^{m}$ are universal and consist of the reference motion cues (or human perceived quantities):

$$
\begin{aligned}
\dot{\delta}^p_{\bar{x}} &= A^p \delta^p_{\bar{x}} + B^p \delta^p_{\bar{u}} \\
\delta^p_{\bar{x}} &= \begin{bmatrix} \delta_u & \delta_w & \delta_\theta & \delta_q \end{bmatrix}^T \\
\delta^p_{\bar{u}} &= \begin{bmatrix} \delta_{\delta_e} & \delta_{\delta_t} \end{bmatrix}^T
\end{aligned} \tag{1}
$$

$$
\begin{aligned}
\dot{\delta}^m_{\bar{x}} &= A^m \delta^m_{\bar{x}} + B^m \delta^m_{\bar{u}} \\
\delta^m_{\bar{u}} &= \begin{bmatrix} \delta_{f_{x_p}} & \delta_{f_{z_p}} & \delta_{q_p} \end{bmatrix}
\end{aligned} \tag{2}
$$

The EMD analysis is made possible by effectively combining the linear dynamic systems of the aircraft and the MCA into a single system which is excited only by the pilot inputs $\delta^p_{\bar{u}}$, as seen in Eq. (3). This is achieved through adding the perturbed specific forces $\delta_{f_{x_p}}$ and $\delta_{f_{z_p}}$ to the aircraft state vector $\delta^p_{\bar{x}}$ which are in turn given as inputs to the MCA dynamics through the A^{mp} matrix. The end result is a new combined system matrix A^c with a corresponding state vector $\delta^c_{\bar{x}}$ [13].

$$
\begin{aligned}
\begin{pmatrix} \dot{\delta}^p_{\bar{x}} \\ \dot{\delta}^m_{\bar{x}} \end{pmatrix} &= \begin{bmatrix} A^p & 0 \\ A^{mp} & A^m \end{bmatrix} \begin{pmatrix} \delta^p_{\bar{x}} \\ \delta^m_{\bar{x}} \end{pmatrix} + \begin{bmatrix} B^p \\ 0 \end{bmatrix} \begin{pmatrix} \delta^p_{\bar{u}} \\ 0 \end{pmatrix} = A^c \delta^c_{\bar{x}} + B^c \delta \bar{u}^c \\
\begin{pmatrix} \delta^p_{\bar{y}} \\ \delta^m_{\bar{y}} \end{pmatrix} &= \bar{y}^c = C^c \delta^c_{\bar{x}} \\
\delta^p_{\bar{y}} &= \begin{bmatrix} \delta_{f_{x_p}} & \delta_{f_{z_p}} & \delta_{q_p} \end{bmatrix} \\
\delta^p_{\bar{y}} &= \begin{bmatrix} \delta_{f_{x_m}} & \delta_{f_{z_m}} & \delta_{q_m} \end{bmatrix}
\end{aligned} \tag{3}
$$

As a result of this formulation of the combined system, the eigenmodes of the simulated vehicle that can be obtained from the A^p matrix are carried over to the combined system matrix A^c. Furthermore, by employing a modal coordinate transformation, as will be explained in Section II.C, the combined aircraft and simulator motion cues (defined in matrix A^c) can be expressed as (potentially complex) eigenvectors related to the original aircraft eigenmodes. This in turn enables a systematic analysis of the degree to which the simulator motion cue eigenvectors are distorted in magnitude and phase with respect to the aircraft motion cues. Through showing the eigenvectors in the complex plane one can investigate the distortions of all dynamics caused by the MCA.

It is important to clarify that the EMD analysis captures *only* the linear dynamics of the *perturbed* human perceived quantities. Therefore the analysis is valid only close to the given initial condition. If it is desired to evaluate a broader region of the flight envelope, EMD must be performed across multiple points which are subsequently connected by techniques such as gain scheduling. In order to simplify the notations for the remainder of the paper, the δ notation is dropped from the states, inputs and outputs.

B. Application to a linear aircraft model

In this paper, the application of EMD in symmetric flight conditions will be studied. They are described with the dimensional symmetric equations of motion, presented in Eq. (4), that originate from classical flight dynamics. There the influence of the aircraft dynamics can be seen through the stability and control derivatives. It must be stated that the aircraft model used in this study is defined in the stability reference frame, indicating that a transformation is required to express the perceived cues in the pilot-aligned body reference frame. The equations of motion can also be represented in a state-space form, which forms the basis for the A^p and B^p matrices in Eq. (1):

$$
\begin{aligned}
-W\cos\theta_0\theta + X_u u + X_w w + X_q q + X_{\delta_e}\delta_e + X_{\delta_t}\delta_t &= m\dot{u} \\
-W\sin\theta_0\theta + Z_u u + Z_w w + Z_{\dot{w}}\dot{w} + Z_q q + Z_{\delta_e}\delta_e + Z_{\delta_t}\delta_t &= m(\dot{w} - qV) \\
M_u u + M_w w + M_{\dot{w}}\dot{w} + M_{\delta_e}\delta_e + M_{\delta_t}\delta_t &= I_{yy}\dot{q} \\
\dot{\theta} &= q
\end{aligned} \tag{4}
$$

As already stated, $\bar{x}^p$ must be further extended by the inclusion of the specific forces as states in order to enable the coupling of both systems. In turn, the A^p matrix is modified to include the necessary equations for the new states.

State representation of f_{x_p} and f_{z_p}

The specific force can be defined as the non-gravitationally induced acceleration [14]. Therefore, the gravity related components must be removed from the first two equations of motion in Eq. (4) to obtain expressions for the specific forces at the centre of gravity:

$$\begin{aligned} f^s_{x_{cg}} &= \frac{X_u}{m}u + \frac{X_w}{m}w + \frac{X_q}{m}q + \frac{X_{\delta_e}}{m}\delta_e + \frac{X_{\delta_t}}{m}\delta_t \\ f^s_{z_{cg}} &= \frac{Z_u}{m}u + \frac{Z_w}{m}w + \frac{Z_{\dot{w}}}{m}\dot{w} + \frac{Z_q}{m}q + \frac{Z_{\delta_e}}{m}\delta_e + \frac{Z_{\delta_t}}{m}\delta_t \end{aligned} \tag{5}$$

However, the MCA requires the specific forces to be defined in the body reference frame. Therefore $f^s_{x_{cg}}$ and $f^s_{z_{cg}}$ must be transformed from the stability frame to the body frame, as demonstrated in Eq. (6). Here α_0 denotes the initial condition for angle of attack in the body reference frame, since, by definition, the initial angle of attack in the stability reference frame is 0. The transformation is not needed if the used aircraft model is already defined in the body reference frame.

$$\begin{aligned} f^b_{x_{cg}} &= f^s_{x_{cg}} \cos\alpha_0 - f^s_{z_{cg}} \sin\alpha_0 \\ f^b_{z_{cg}} &= f^s_{z_{cg}} \cos\alpha_0 + f^s_{x_{cg}} \sin\alpha_0 \end{aligned} \tag{6}$$

The final step to arrive at the complete expressions is to move the specific forces to the pilot station. This is an important requirement for the EMD implementation for fixed-wing aircraft, and in contrast to the application of the method in rotorcraft, where the cues can typically be evaluated at the vehicle centre of gravity (CG) [13]. In fixed-wing aircraft the pilot is often located a large distance in front of the CG, which is quantified by the horizontal and vertical cockpit moment arms l_x and l_z, see Fig. 1. Together with the pitch rotation acceleration these arms can considerably affect the specific forces perceived by the pilot from the ones at the centre of gravity as shown in Fig. 1 and Eq. (7). The extent to which this happens depends on the evaluated aircraft type. For example this effect will be more pronounced on an airliner than on a business jet, since the former aircraft tend to have larger cockpit moment arms than the latter.

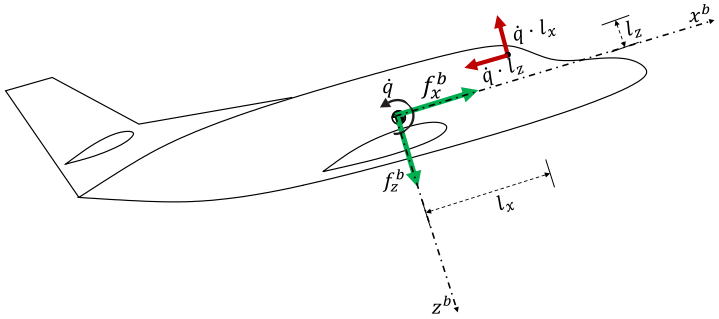

Fig. 1 Influence of the pitch acceleration on the specific forces at the pilot position

$$\begin{aligned} f_{x_p} &= f^b_{x_{cg}} - \dot{q} l_z \\ f_{z_p} &= f^b_{z_{cg}} - \dot{q} l_x \end{aligned} \tag{7}$$

To arrive at the state-space representation of f_{x_p} and f_{z_p}, their time derivative is found by differentiating their expressions obtained from combining Eqs. (5) to (7). In this process the time derivatives of the pilot inputs δ_e and δ_t are found by

approximating their associated actuator dynamics as a first order lag filter as demonstrated in Eqs. (8) and (9). There $\delta_{u_{e/t}}$ stands for the pilot input for the elevator or thrust setting, while $\tau_{e/t}$ is the corresponding time constant. The actuator dynamics approximation results in δ_e and δ_t being moved to the vehicle state vector and δ_{u_e} and δ_{u_t} form the new input vector.

$$H_{\delta_{e/t}} = \frac{1}{\tau_{e/t}s + 1} \tag{8}$$

$$\dot{\delta}_{e/t} = \delta_{u_{e/t}} - \frac{1}{\tau_{e/t}}\delta_{e/t} \tag{9}$$

It must be stated that the values of the time constants $\tau_{e/t}$ have no influence on the final eigenvector distortions of the motion cues. This behaviour is expected, since even though the actuator dynamics affect the aircraft motion cues, the latter are used only as the inputs in the MCA dynamics and therefore have no influence on them. However, in the specific case that the MCA also uses δ_e and δ_t as inputs, the values of $\tau_{e/t}$ must be selected to represent the simulated aircraft and flight condition. In the current analysis, the MCA does not rely on the pilot inputs and $\tau_{e/t} = 0.01$.

This concludes the derivation of the state-space representation of f_{x_p} and f_{z_p}. The resulting aircraft state and input vectors $\bar{x}^p$ and $\bar{u}^p$ are presented in Eq. (10) together with the total system output, vector $\delta^p_{\bar{y}}$.

$$\begin{aligned}
\bar{x}^p &= \begin{bmatrix} u & v & w & \theta & q & \delta_e & \delta_t & f_{x_p} & f_{z_p} & \dot{q} \end{bmatrix}^T \\
\bar{u}^p &= \begin{bmatrix} \delta_{u_e} & \delta_{u_t} \end{bmatrix}^T \\
\bar{y}^p &= \begin{bmatrix} q & f_{x_p} & f_{z_p} \end{bmatrix}^T
\end{aligned} \tag{10}$$

Coupling of the two systems

In this study, the used MCA is the Classical Washout Algorithm (CWA) [14], shown in Fig. 2. Since only the longitudinal motions will be analyzed, it is assumed that $\phi_m = \psi_m = 0°$. Furthermore, in the linearization process small angle approximations are used and the rate limit of the platform tilt coordination is not modelled.

The coupling of the aircraft and MCA linear systems is done through the A^{mp} matrix as was previously stated. Because the aircraft motion cues are present in its state vector, the A^{mp} can be directly constructed from the simulator input matrix B^m. The same process is repeated for the construction of the coupled system output matrix C^c, where C^{mp} effectively binds the MCA outputs to the aircraft dynamics, as seen in Eq. (11). The definitions for A^{mp} and C^{mp} are in turn shown in Eq. (12), in which D^m represents the MCA feedthrough matrix.

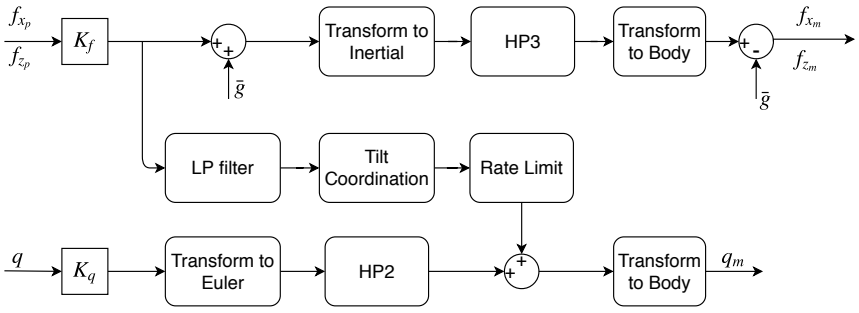

Fig. 2 The Classical Washout Algorithm adapted for longitudinal motions [14]

$$C^c = \begin{bmatrix} C^p & 0 \\ C^{mp} & C^m \end{bmatrix} \tag{11}$$

$$A^{mp} = [0 \quad B^m] \qquad C^{mp} = [0 \quad D^m] \tag{12}$$

C. Distorted eigenvector analysis

The final component of the EMD methodology is finding the extent of the distortion of the aircraft motion cues by the MCA dynamics. The combined system formulation presented in Eq. (3) enables the representation of the perceived motion cues as components of the eigenvectors of the A^c matrix, which also describe the vehicle dynamic modes. In Eq. (10) it can be observed that the aircraft motion cues f_{x_p}, f_{z_p}, and q are already part of $\bar{x}^p$ and are thus represented in the eigenvectors of A^c. The same, however, is not valid for the motion cues in the simulator f_{x_m}, f_{z_m}, and q_m. As a result of the system coupling, these are expressed as a combination of aircraft and simulator states, which is observed in Eqs. (3), (11) and (12). Thus, in order to relate the simulator motion cues to the vehicle dynamic modes a *modal coordinate transformation* needs to be performed [17].

The modal coordinate transformation is in principle a change of basis of the system defined by A^c,B^c,C^c and D^c matrices. This is done with the help of the modal matrix V, defined in Eq. (13), where V contains the right eigenvectors of A^c corresponding to the eigenvalues λ_c [17]:

$$A^c V = \lambda_c V \tag{13}$$

In general it is assumed that there are n distinct eigenvalues, thus making V invertible. This assumption is valid for the current formulation of A^c. The modal matrix is used to define a new state vector – the modal state $\bar{z}$ and corresponding matrices, presented in Eqs. (14) to (17):

$$\bar{z} = V^{-1}\bar{x}^c \tag{14}$$

$$\dot{\bar{z}} = (V^{-1}A^cV)\bar{z} + (V^{-1}B^c)\bar{u}^c \tag{15}$$

$$\bar{y}^c = (C^cV)\bar{z} = C_{mod}\bar{z} \tag{16}$$

$$C_{mod} = \begin{bmatrix} f_{x_{p_{mod}}} & f_{z_{p_{mod}}} & q_{mod} & f_{x_{m_{mod}}} & f_{z_{m_{mod}}} & q_{m_{mod}} \end{bmatrix}^T \tag{17}$$

The new modal output matrix C_{mod} contains the motion cue components of all eigenvectors of A^c expressed in terms of the modal state $\bar{z}$ as shown in Eq. (16). The simulator-related entries in C_{mod} are therefore connected to the dynamic modes of the aircraft through $\bar{z}$. For the aircraft-related motion cues the rows in C_{mod} are equivalent to rows in V, which correspond to f_{x_p}, f_{z_p} and q. The end result is that it is possible to do a direct comparison between the motion of the aircraft and the motion cues produced by the simulator, all expressed as eigenvectors of the combined system. The comparison is then visualized by plotting all motion cue eigenvectors in the complex plane.

An example visualization of the distorted eigenvectors is presented in Fig. 3, where the used MCA is taken from [18] and is applied on a Cessna Citation 500 linear model. The solid and dashed lines represent the motion cue eigenvector components of, respectively, the aircraft and the simulator. The eigenvectors in Fig. 3a and Fig. 3b in turn correspond to the eigenvalues of the short period and phugoid eigenmodes. The aircraft related eigenvectors have different magnitude and phase relations to one another that originate from the aircraft model. Therefore they remain fixed and do not change with the MCA parameters. The relations between the MCA related eigenvectors change when altering the MCA parameters.

It is important to note that the comparison of eigenvector magnitudes can only be made for the same motion cues due to their different dimensions. For example in Fig. 3 it can be seen that f_{z_p} has a much higher amplitude than q_p for both eigenmodes. However, it would be wrong to conclude that f_{z_p} is a more dominant motion cue than q_p in these eigenmodes.

The magnitude distortion of an eigenvector can be defined as the ratio of the magnitudes of the simulator eigenvector with respect to the aircraft eigenvectors. For example, in Fig. 3a it is observed that $|f_z|_{sp} = \frac{|f_{z_m}|_{sp}}{|f_{z_p}|_{sp}} = 0.73$. Similarly,

the phase distortion is characterised by the angle between the aircraft and simulator eigenvector. If the eigenvectors corresponding to the positive conjugate eigenvalues are visualized, counter-clockwise and clockwise phase distortions indicate, respectively, phase lead and phase lag. For example in Fig. 3a f_{z_m} has a phase distortion of 87 degrees counter-clockwise ($\angle(f_z)_{sp} = 87°$ lead), while q_m has a 13 degree clockwise distortion in phase ($\angle(q)_{sp} = 13°$ lag). The magnitude distortion for q_m is pronounced with $|q|_{sp} = 0.43$, while f_{x_m} has a good level of magnitude and phase distortions: $|f_x|_{sp} = 0.77$, and $\angle(f_x)_{sp} = 33°$ lead.

The eigenvector distortions can also be seen in the time domain. Consider that a system is excited with eigenmode i, which is described by a pair of complex conjugate eigenvectors v_i and v_i^*. This is visualized in the time domain through the zero-input response of the system to an initial condition of $2Re(v_i)$. The distortions related to the short period are presented in Fig. 4a. Here it can be observed that f_{x_m} is slightly leading f_{x_p} while having a slightly lower amplitude, corresponding with the eigenvector distortions. Similar observations that correlate to Fig. 3a can be made for f_z and q.

The EMD analysis for the phugoid is presented in Fig. 3b. Immediately it is noticeable that the pitch and heave motion cues in the simulator are almost non-existent: $\angle(f_z)_{phug} = 108°$ lag, $|f_z|_{phug} = 5.65 \cdot 10^{-4}$ and $\angle(q)_{phug} = 101°$ lag, $|q|_{phug} = 0.097$. The surge cues are less distorted: $\angle(f_x)_{phug} = 16°$ lag, $|f_x|_{phug} = 0.71$. The time domain representation of the phugoid distortions is shown in Fig. 4b, where f_{z_m} and q_m are essentially zero.

Finally, the modal coordinate transformation results in a parameter presenting the modal response of the system in the time domain. This is the absolute value of the complex modal state $\bar{z}$ that gives information on the participation of each mode in the system response [13]. This measure is called a *Mode Participation Factor* (MPF) and its integrated value over a given time gives an indication of the relative contribution of each mode in a particular manoeuvre.

D. Proposed criteria for filter tuning

The currently proposed tuning approach used with EMD aims to preserve the aircraft motion cues in the simulator for one eigenmode of choice while using as much as possible from the available motion space. This is achieved by tuning with the following criteria shown in their order of importance:

1) Minimize the phase distortions of all motion cues.
2) Maintain the relative phases between the motion cues. This effectively translates to all motion cues having phase lag or phase lead distortions of similar proportions.
3) Minimize the magnitude distortions of all motion cues.
4) Attempt to maintain a similar magnitude distortion level for all motion cues.

After the tuning process is completed, it needs to be checked whether motion platform exceeds the available motion space for a desired task or manoeuvre. If the space is exceeded, the tuning process is repeated until the actuator length limits are no longer reached.

Finally, it must be stated that these criteria used for tuning are not necessarily optimal and are based on the current interpretation of EMD. Future research might prove that better approaches exist.

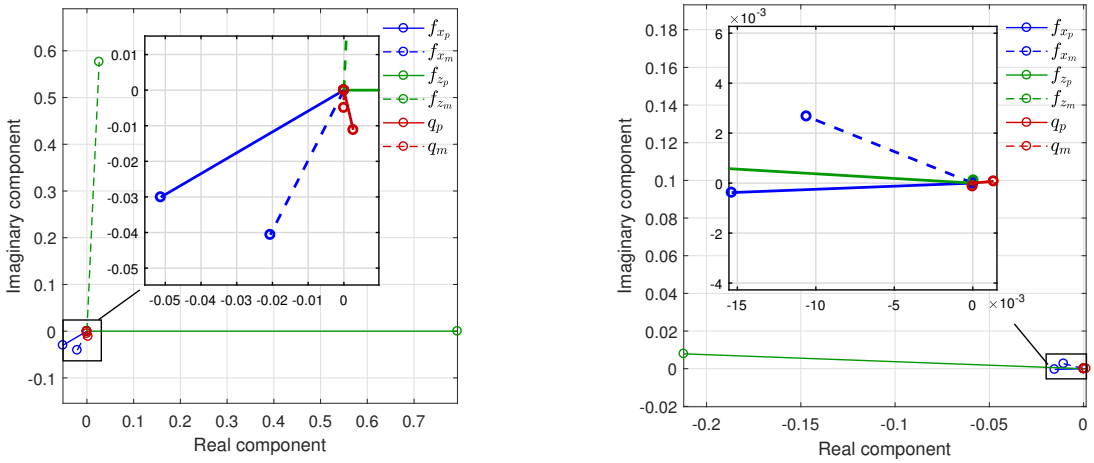

(a) Short Period, $\lambda_{sp} = -2.0362 \pm 3.0513i$

(b) Phugoid, $\lambda_{ph} = -0.0124 \pm 0.1149i$

Fig. 3 Example for eigenvector distortion plots

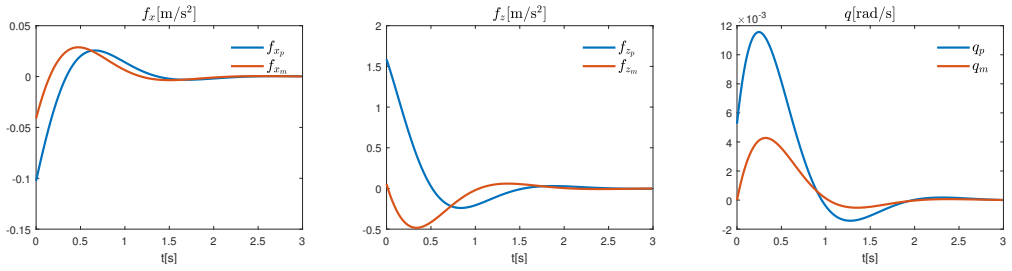

(a) Short period eigenmode

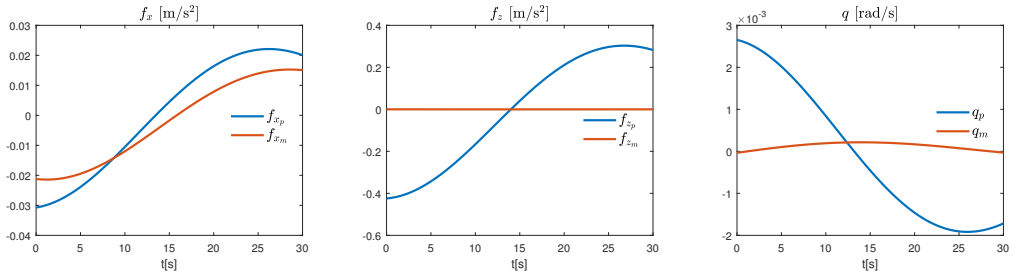

(b) Phugoid eigenmode

Fig. 4 Time histories of separately exciting the two eigenmodes of the aircraft

III. Practical application of EMD and comparison to OMCT

In this study the EMD analysis is applied to a linear model of the Cessna Citation 500 in cruise configuration, which is presented in Table 1. The goal is to arrive at configurations which accurately simulate one of the two eigenmodes.

Table 1 The Cessna Citation I (dimensionless) linear model parameters

C_{X_0}	= -0.0277	C_{Z_0}	= -0.216	C_{m_0}	= 0.213	m	= 5207 [kg]
C_{X_u}	= -0.0698	C_{Z_u}	= -0.4702	C_{m_u}	= 0.0561	S	= 24.2 [m^2]
C_{X_α}	= 0.0744	C_{Z_α}	= -5.6149	C_{m_α}	= -0.4982	$\bar{c}$	= 2.022 [m]
$C_{X_{\dot{\alpha}}}$	= 0.0259	$C_{Z_{\dot{\alpha}}}$	= -0.2039	$C_{m_{\dot{\alpha}}}$	= 0.1689	V	= 160.03 [m/s]
C_{X_q}	= -0.4179	C_{Z_q}	= -5.8339	C_{m_q}	= -10.152	h	= 5000 [m]
$C_{X_{\delta_e}}$	= -0.0131	$C_{Z_{\delta_e}}$	= -0.5814	$C_{m_{\delta_e}}$	= -1.2269	ρ	= 0.7361 [kg/m^3]
$C_{X_{\delta_t}}$	= 0	$C_{Z_{\delta_t}}$	= 0	$C_{m_{\delta_t}}$	= 0	K_{YY}	= 1.114 [-]

The short period eigenmode is selected for tuning of the configurations. It is preferred to the phugoid since motion simulators are better suited to emulating high-frequency accelerations than ones of low-frequency due to the limited motion space [14]. Furthermore, magnitude and phase distortions become more prominent during precision control tasks and do not influence the fidelity of large amplitude manoeuvres [19]. The short period eigenmode is a better representative of the former. Moreover, in order for the phugoid to be the dominant eigenmode in a manoeuvre a large deviation from the initial trim condition is needed. This can lead to leaving the validity region of the EMD method, which analyses the linear dynamics of the system state and input *perturbations*. Finally, the distortions related to the short period exhibit noticeable variations with changing CWA parameter configurations, while the distortions for the phugoid remain similar to the behaviour observed in Fig. 3b with severely attenuated heave and pitch motion cues.

In total four CWA configurations, presented in Tables 2 and 3, were analyzed. The baseline configuration B is tuned based on established rules of thumb and previous experience from motion tuning experiments on the SRS. Furthermore, it is ensured that this configuration complies to the current OMCT criteria set in ICAO 9625 [10]. The next two configurations $E_{ph(ase)}$ and $E_{m(agnitude)}$ are tuned according to the EMD analysis approach. The difference between the two is that E_{ph} has the smallest phase distortion for f_x and q, while E_m has the smallest overall magnitude distortion summed over all motion cues. The final configuration O is tuned to pass the current OMCT tests while exhibiting unsatisfactory behaviour in the EMD analysis. For all configurations, a pull-up push-over manoeuvre of $\pm 5^\circ$ pitch angle capture was simulated to ensure that the available motion space was not exceeded. The result from these simulations is that all configurations were set with the same heave parameters, as the heave cue is largely uncoupled from the other degrees of freedom, and the most motion space is used up in replicating the heave movements. Furthermore, all subsequent performance differences are resulting from the settings for the coupled pitch and surge axes. Therefore from now on when magnitude and phase distortions are discussed, this is done for f_x and q unless specifically stated otherwise.

Table 2 Labels and description of the four used configurations of the Classical Washout Algorithm

Label	Description
B	Baseline configuration, complying with the OMCT criteria.
O	OMCT tuned configuration with bad performance in EMD, complying with the OMCT criteria.
E_{ph}	Configuration with smallest phase distortion, not complying with the OMCT criteria.
E_m	Configuration with the smallest magnitude distortion, not complying with the OMCT criteria.

Table 3 Classical Washout Algorithm filter parameters for all configurations used in the experiment

	K_x [-]	ω_{n_x} [rad/s]	ω_{b_x} [rad/s]	$\omega_{n_{lpx}}$ [rad/s]	ζ_x [-]	K_z [-]	ω_{n_z} [rad/s]	ω_{b_z} [rad/s]	ζ_z [-]	K_q [-]	ω_{n_q} [rad/s]	ζ_q [-]
B	0.7	0.8	0	2.5	1	0.5	2.5	0.2	1	0.7	0.8	1
O	0.7	2	0	4	1	0.5	2.5	0.2	1	0.7	1	1
E_{ph}	0.8	1	0	1	1	0.5	2.5	0.2	1	0.7	0.7	1
E_m	0.8	1.5	0	1	1	0.5	2.5	0.2	1	0.7	1	1

The eigenvector distortion plots for all configurations are shown in Fig. 5 with their distortions quantified in Table 4. By inspecting them it can be observed that configurations E_{ph} and E_m maintain fairly low phase distortions while attempting to keep the relative phase between f_x and q as inherent in the aircraft dynamics. The baseline configuration B exhibits reasonable phase and magnitude distortions. However, the relative phase is not preserved, as q is exhibiting phase lag, while f_x shows a phase lead distortion. A similar behaviour is observed in configuration O, where the phase distortion in f_x and magnitude distortion in q are prominent.

These trends are also evident in the time-domain representation of the distortions, presented in Fig. 6. For instance, note how f_{x_m} is out of phase with respect to f_{x_p} at $t = 0$ for configuration O, see Fig. 6b. This corresponds to its phase distortion of $\angle(f_x)_{sp} = 152.1°$ lead. In the same figure, it is clearly visible that q_m has a higher amplitude than q_p and is lagging behind it, which is again in accordance with the eigenvector distortion results.

The excitation of the eigenmodes also aids in the understanding of how the MPFs behave. In Fig. 7a it can be observed that when the initial condition is the short period eigenvector, the SP MPF component starts from one and quickly reduces to zero. The opposite is seen in Fig. 7b, when the phugoid eigenvector is the initial condition, where the phugoid MPF gradually decreases while the aircraft is returning to its trimmed state. For both conditions, the MPF of the eigenmode that is not excited is verified to have a value zero throughout the entire evaluation. This behaviour is directed by the short period and phugoid eigenvalues (λ_{sp} and λ_{ph}), presented in Eq. (18), which govern the frequency and damping of both eigenmodes:

$$\lambda_{sp} = -2.0362 \pm 3.0513i \qquad \lambda_{ph} = -0.0124 \pm 0.1149i \tag{18}$$

While methods such as EMD and OMCT are usually used for evaluation of the motion cueing fidelity they can also be employed for tuning of the MCA. For example De Ridder and Roza [11] investigated an automatic tuning method using OMCT. The four CWA configurations used in the current study enable the presentation of both tuning and evaluation using EMD. For the former, configurations E_{ph} and E_m are tuned to produce motion cues at *least* as good as the baseline B, in terms of subjective pilot opinion. It is hypothesized that this statement is valid, since configurations E_{ph} and E_m have similar or lower phase and magnitude distortions than the baseline B, as seen in Table 4.

For the evaluation, a ranking can be made based on interpreting the outcome of the EMD analysis with respect to the tuning criteria and their relative importance, that are set in Section II.D. This ranking for the presented configurations is $E_{ph} > E_m > B > O$. Configuration E_{ph} has the lowest phase distortion for surge and pitch, while simultaneously maintaining reasonably low magnitude distortions. E_m has on average better magnitude distortions, but a slightly worse phase distortions which ranks it on second place. The baseline configuration B has worse phase distortions and magnitude than E_{ph} and E_m. Furthermore it fails to preserve the relative phase between f_{x_p} and q_p, since f_{x_m} has a phase lead distortion, while q_m has a phase lag distortion. Configuration O has the same problem, which is even more pronounced due to the large phase lead distortion of f_{x_m}. This, combined with it having the largest magnitude distortion for q_m, gives it the last place in the EMD based ranking.

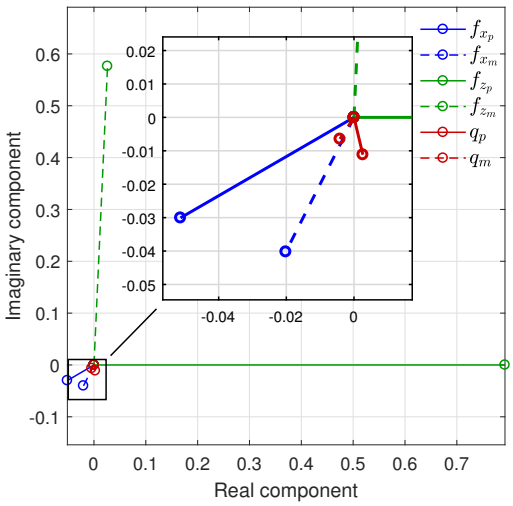

(a) Configuration B

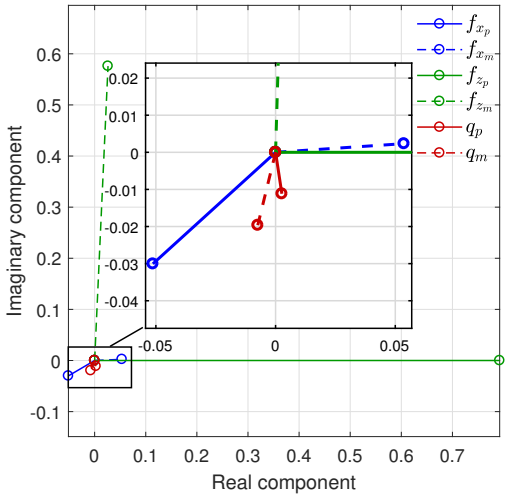

(b) Configuration O

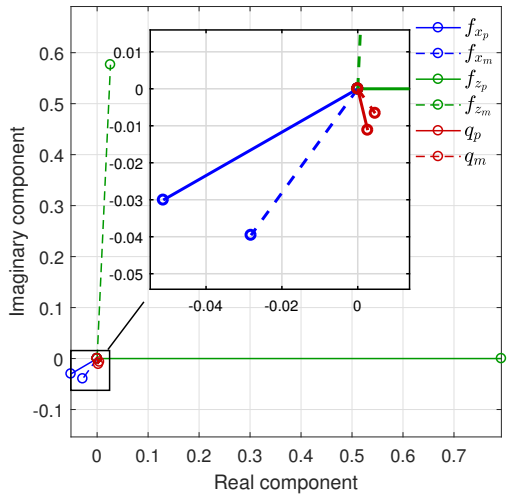

(c) Configuration E_{ph}

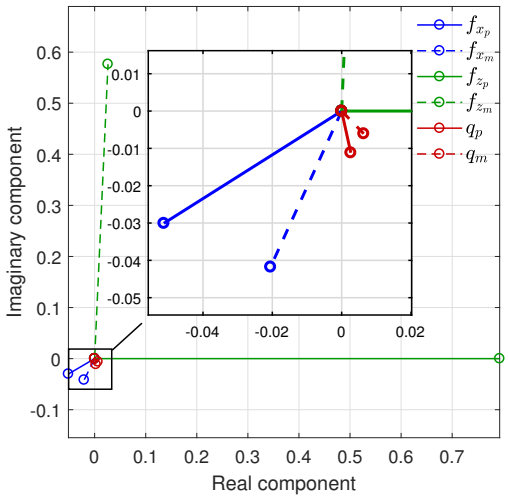

(d) Configuration E_m

Fig. 5 Short period eigenvector distortion plots for all CWA configurations

Table 4 Short period eigenvector magnitude and phase distortions for all CWA configurations

	$\lvert f_x \rvert_{sp}$	$\angle(f_x)_{sp}[^\circ]$	$\lvert f_z \rvert_{sp}$	$\angle(f_z)_{sp}[^\circ]$	$\lvert q \rvert_{sp}$	$\angle(q)_{sp}[^\circ]$
B	0.76	33.0 lead	0.73	87.4 lead	0.67	45.9 lag
O	0.90	152.1 lead	0.73	87.4 lead	1.83	34.0 lag
E_{ph}	0.82	24.2 lead	0.73	87.4 lead	0.70	21.6 lead
E_m	0.78	33.5 lead	0.73	87.4 lead	0.76	33.1 lead

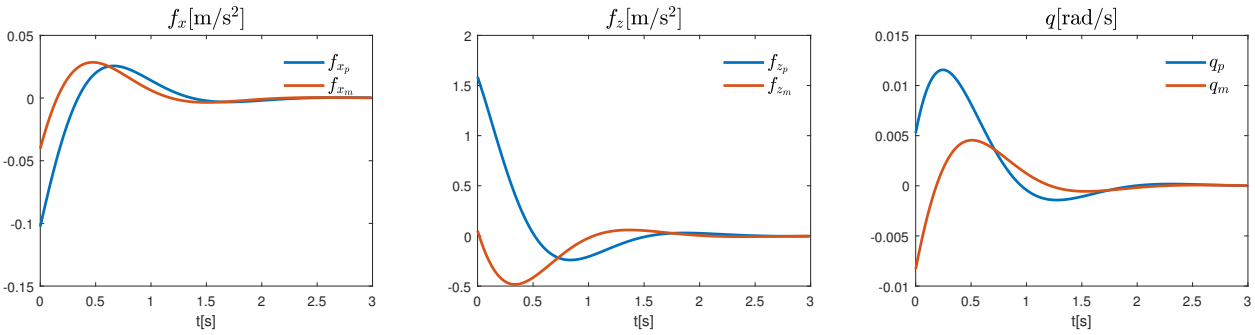

(a) B

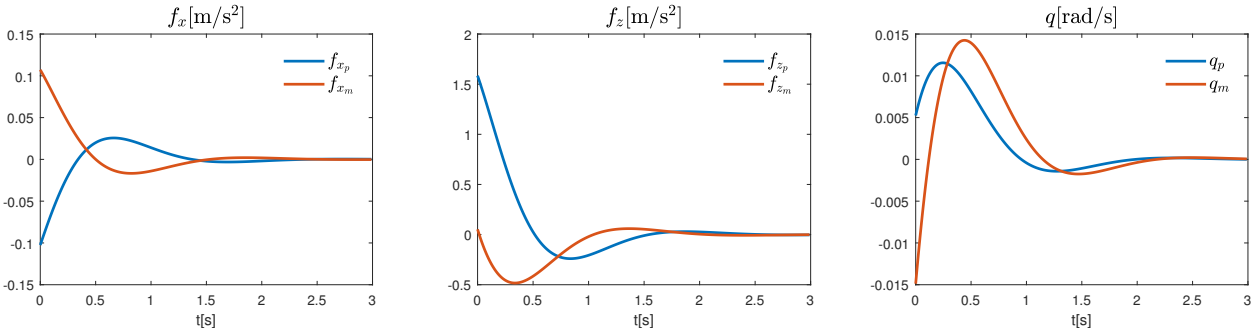

(b) O

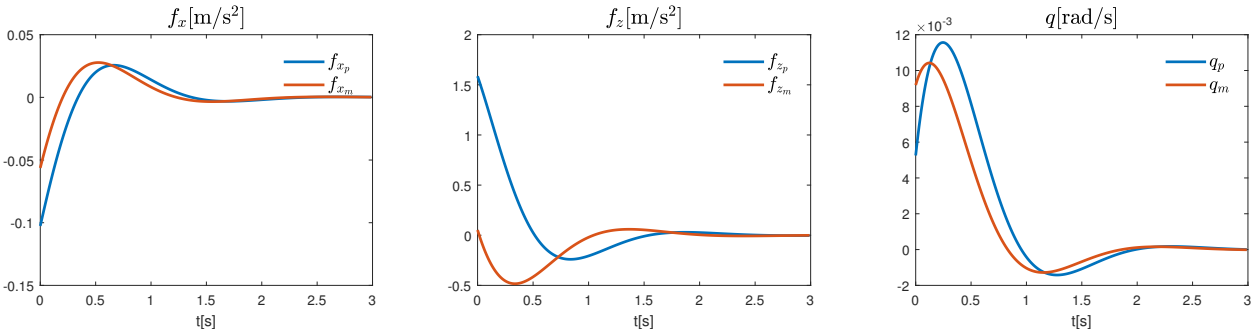

(c) E_{ph}

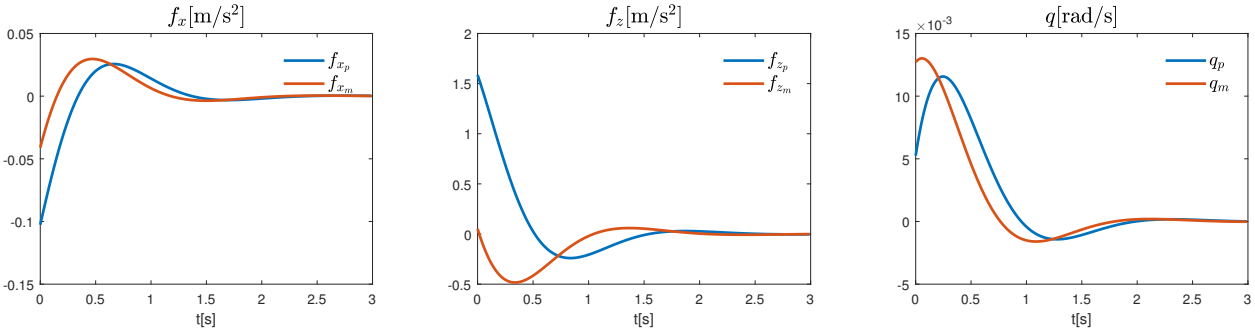

(d) E_m

Fig. 6 System response to the short period eigenmode excitation

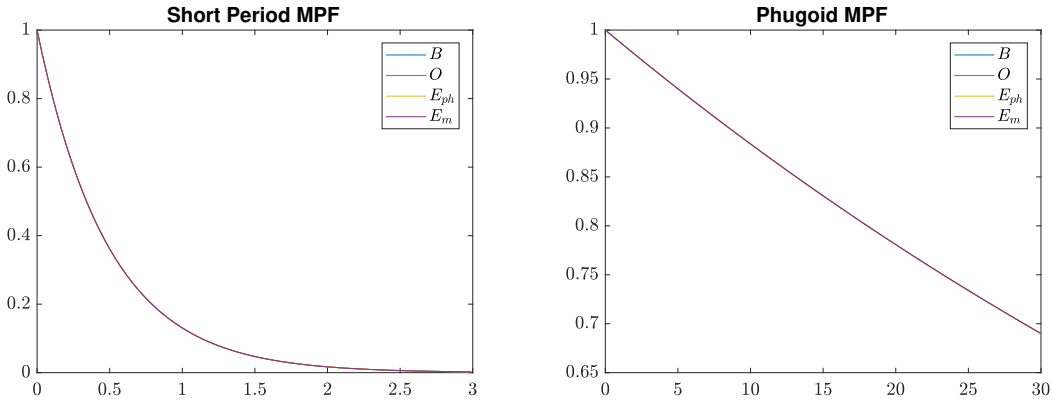

(a) Short Period initial condition **(b) Phugoid initial condition**

Fig. 7 MPF evolution for the system response to both eigenvector initial conditions

The four CWA configurations are also subjected to offline OMCT tests excluding the dynamics of the motion platform [18]. Their results are presented in Fig. 8 where the fidelity boundaries are the ones defined in ICAO 9625 [10]. As previously stated, configurations B and O manage to comply to the OMCT conditions. It is also observed that B manages to stay within the boundaries a bit better than O, since for the latter in surge test 6 the magnitude at $\omega = 1.585$rad/s lies just outside the lower boundary.

The frequency response of the EMD tuned configurations E_{ph} and E_m lies outside these boundaries for almost the entire tested frequency range for pitch test 1 and for its lower half for surge test 6 as observed in Fig. 8a. Furthermore, E_m lies further away from the fidelity boundaries than E_{ph} for both the pitch and surge tests. Therefore, a ranking based on the OMCT results can also be devised: $B > O > E_{ph} > E_m$.

Even though the two rankings overlap in the sense that in both $B > O$ and $E_{ph} > E_m$, they exhibit enough differences for the used configurations. The validity of both rankings can be tested in a piloted experiment.

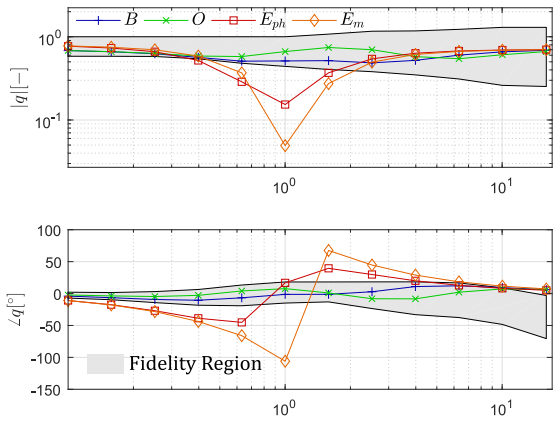

(a) Pitch due to pitch (test 1)

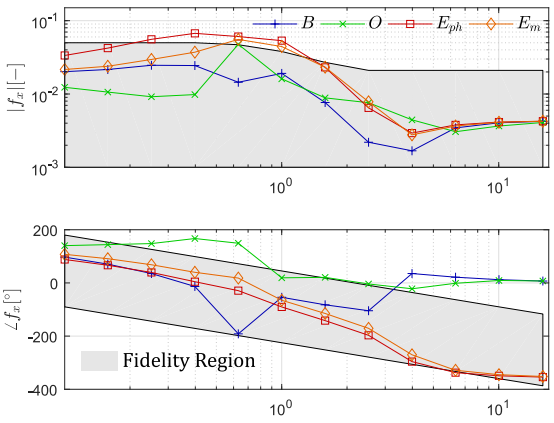

(b) Surge due to pitch (test 2)

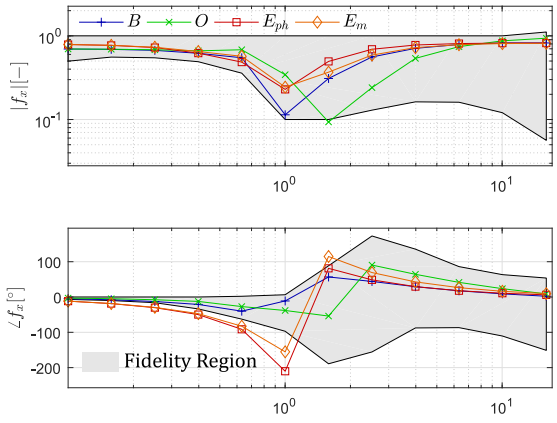

(c) Surge due to surge (test 6)

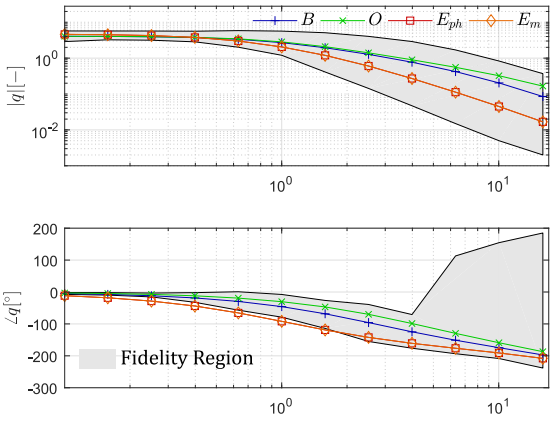

(d) Pitch due to surge (test 7)

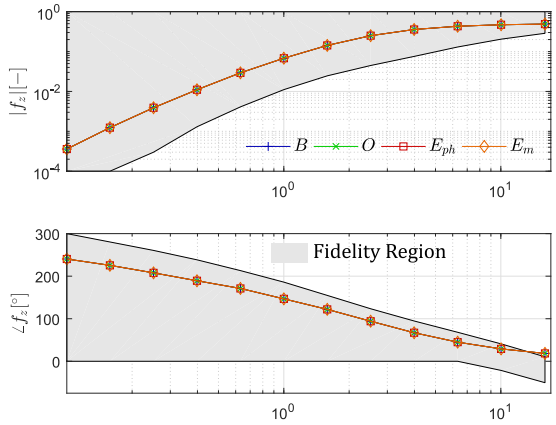

(e) Heave due to heave (test 10)

Fig. 8 OMCT results for all configurations

IV. Experiment set up

In order to investigate the predictive capabilities of the EMD methodology and to validate its inherent assumptions, a pilot-in-the loop experiment is performed in the SIMONA Research Simulator (SRS). The used MCA configurations are the ones presented in Table 2, while the simulated aircraft is a non-linear high-fidelity model of the Cessna Citation 500 business jet. The initial trim condition is at an altitude of 5000m and Mach number of 0.5 with the corresponding velocities V_{TAS} = 160 m/s and V_{IAS} = 245 kts. Six pilots of different background performed double-blind pairwise comparisons between all four CWA configurations by exciting the aircraft short period dynamics. This section will present the a-priori hypothesis, followed by a discussion of the task flown by the pilots, the experimental structure, and a brief description of the participants.

A. Hypothesis

The main experiment hypothesis is that EMD is a better predictor of the subjective motion cueing fidelity given by pilots for motions exciting the aircraft short period oscillation dynamics than OMCT. An alternative formulation is that the EMD-based ranking will better correspond to the winners of the pairwise comparisons than the OMCT-based ranking.

B. Experiment Task

The task of the evaluation pilots is to excite the aircraft and subsequently the simulator motion system in a way allowing them to confidently state a preference for the most realistic condition in the evaluated pair. Pilots are instructed to excite the aircraft short period dynamics as they wish, on the condition that they obey the following boundaries:

- The airspeed must not deviate more than ±10 knots from the trim airspeed.
- Any pitch captures that are performed must not exceed ±5°.
- No full deflections of the side stick are allowed.
- Different strategies for exciting the short period can be tried during training, but only a single strategy can be used during the evaluation runs.

There are several reasons for these limitations. First, the aircraft must not deviate too much from the trimmed condition, since the motion filters are specifically tuned for it. Second, large pitch inputs must be avoided since it is easy to overstress the simulated aircraft and quickly run out of available motion space due to excessive heave. An additional measure to prevent this is the implementation of a force curve on the side stick identical to the one used in the Airbus A320 in a cruise configuration. The strategy must remain consistent to ensure that any perceived differences in the simulator motion are resulting only from the evaluated CWA configurations.

Pilots are also provided with a full outside visual, and a Primary Flight Display (PFD) to monitor the airspeed and pitch angle. In addition, an engine noise is played while the pilots were performing the task in order to mask any noise coming from the hydraulic motion actuators. Finally, the roll and yaw controls are disabled.

C. Experiment Structure

Dependent measures

The main recorded variable is the preferred CWA configuration from each paired comparison. Pilots are briefed to select the 'winner' as the configuration which presents the most realistic motion cues. For validation purposes, time histories of the pilot inputs, aircraft states and specific forces, and the simulation motion cues are recorded.

Training

Each pilot is subjected to approximately 20 minutes of training. In this phase, the pilots fly all four CWA configurations two times in a randomized order. Every training run lasts for one minute, during which a pilot can explore different

control strategies that enable him to make an evaluation of the motion cueing fidelity. All pilots are instructed to choose a single strategy by the end of the training and keep using it in the evaluation phase.

There are two additional training runs in the form of a standard pair comparison that are done immediately after a short break.

Evaluation phase

The evaluation phase begins after the training has concluded. The pilots first perform all six paired comparisons once. After a break, the paired comparisons are repeated with the CWA configurations presented in the opposite order. The Latin square matrix of all configurations is presented in Table 5.

Table 5 Latin Square matrix of the experiment conditions for all pilots

Subject	Conditions											
1	$B-O$	$B-E_{ph}$	E_m-E_{ph}	$B-E_m$	E_m-O	$O-E_{ph}$	$E_{ph}-O$	$O-E_m$	E_m-B	$E_{ph}-E_m$	$E_{ph}-B$	$O-B$
2	$B-E_{ph}$	$B-E_m$	$B-O$	$O-E_{ph}$	E_m-E_{ph}	$O-E_m$	E_m-O	$E_{ph}-E_m$	$E_{ph}-O$	$O-B$	E_m-B	$E_{ph}-B$
3	$B-E_m$	$O-E_{ph}$	$B-E_{ph}$	$O-E_m$	$B-O$	$E_{ph}-E_m$	E_m-E_{ph}	$O-B$	E_m-O	$E_{ph}-B$	$E_{ph}-O$	E_m-B
4	$O-E_{ph}$	$O-E_m$	$B-E_m$	$E_{ph}-E_m$	$B-E_{ph}$	$O-B$	$B-O$	$E_{ph}-B$	E_m-E_{ph}	E_m-B	E_m-O	$E_{ph}-O$
5	$O-E_m$	$E_{ph}-E_m$	$O-E_{ph}$	$O-B$	$B-E_m$	$E_{ph}-B$	$B-E_{ph}$	E_m-B	$B-O$	$E_{ph}-O$	E_m-E_{ph}	E_m-O
6	$E_{ph}-E_m$	$O-B$	$O-E_m$	$E_{ph}-B$	$O-E_{ph}$	E_m-B	$B-E_m$	$E_{ph}-O$	$B-E_{ph}$	E_m-O	$B-O$	E_m-E_{ph}

For every pair, one evaluation run of maximum one minute is performed for each CWA configuration. The pilots can stop the run once they feel that they sufficiently know the motion signature of the condition.

Test subjects

Six pilots with a varying degree of experience participated in the piloted experiment. All of them gave their informed consent prior to starting the experiment. Their background is summarized below:

- *Subject 1* - Retired military test pilot with experience in motion simulation experiments.
- *Subject 2* - Active general aviation pilot.
- *Subject 3* - Active aerobatic glider pilot experienced in motion cueing evaluation of Level-D Full Flight Simulators (FFS).
- *Subject 4* - Active Cessna Citation 550 research pilot with experience in motion simulation experiments.
- *Subject 5* - Active test pilot of commercial airliners with experience in motion simulation experiments.
- *Subject 6* - Active airline pilot and Cessna Citation 550 research pilot with experience in motion simulation experiments.

V. Results

The results for all pairwise comparisons grouped for all subjects is presented in Fig. 9. The height of bars represents the total number of times this configuration has been preferred in this current pair. The different colours correspond to the evaluations given by each subject. It must be noted that there is one missing data point for the pair $B-E_m$ as Subject 1 was unable to give a confident preference in one of his evaluations.

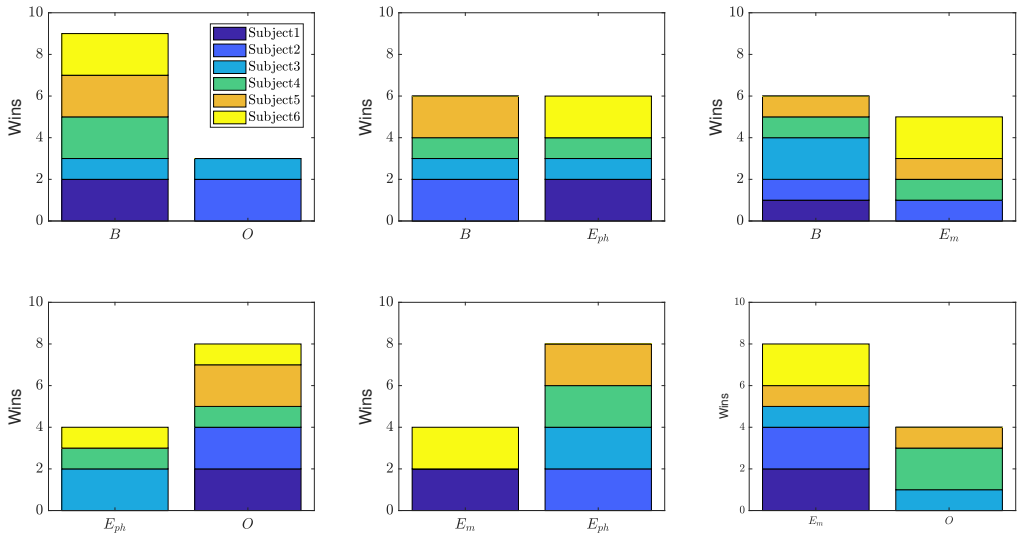

Fig. 9 Results of the pairwise comparisons for all pairs evaluated by all pilots

In Fig. 9 it can be observed that the subjects express two types of consistency. The first is the *within-pair* consistency which is satisfied when the same configuration is preferred in both evaluations of a given pair, visualized by a full bar in Fig. 9. It is seen that for the pair $E_{ph} - E_m$ all subjects are within-pair consistent. The second consistency type is related to the *transitivity* of the evaluations from the different pairs. An example of a perfectly transitive evaluation is when $B > O$, $O > E_{ph}$, $E_{ph} > E_m$, and $O > E_m$. When the data for all pilots are analyzed, it can be concluded that it is intransitive, since a circular triad is present: $O > E_{ph}$, $E_{ph} > E_m$, but $E_m > O$. This prevents the formulation of a clear and intuitive ranking based on the absolute results from all pilots for every pair.

However, it is possible to use statistical modelling techniques in order to arrive at an estimation of a data-based ranking. Many methods exist for statistical analysis of paired comparisons data which is likely to have high degree of dependence [20], as is the case with the evaluations of a repeated measures experiment. One approach is to fit the data to a Bradley-Terry pattern model with the *R* package **`prefmod`** [21]. The model assumes that the evaluations made by a single pilot are dependent, while the evaluations of the different pilots are independent. The resulting ranking is $B > E_{ph} > E_m > O$ with corresponding worth parameters $\left\{\pi_B, \pi_{E_{ph}}, \pi_{E_m}, \pi_O\right\} = \left\{0.348, 0.335, 0.174, 0.143\right\}$. There are other methods that can provide more accurate models which are better tailored to the specific data [20]. Their implementation is unfortunately not straightforward [20] and considerable time would have to be spend on it.

From further analysis of Fig. 9 it is seen that the subjects can be divided in three groups based on their consistency. The first group, formed by Subjects 1 and 2, is within-pair consistent (5 out of 6 pairs) but not transitivity consistent. The second group, represented by Subjects 3 and 4, is the worst with respect to within-pair consistency (3 out of 6 pairs) but is transitively consistent when discarding the inconsistently rated pairs. The third group of Subjects 5 and 6 is both within-pair consistent (with respectively 4/6 and 5/6 pairs) and transitively consistent.

The experiment hypothesis is tested by comparing the ratio of correct paired comparison outcome predictions to the EMD-based ranking and the OMCT-based ranking. Since the two predictors have a degree of similarity - both state that $B > O$ and $E_{ph} > E_m$, the analysis is done for all outcomes as well as the truly discriminatory outcomes (from pairs $B - E_{ph}$, $B - E_m$, $O - E_{ph}$, $O - E_m$), which are indicated as EMD* and OMCT*. These ratios are visualized through box plots in Fig. 10. The data points for each test subject are shown as circles and overlaid on top of the box plots in order to provide a good representation of the data distribution. The colours used for the data points representing the subjects correspond to the legend in Fig. 9. It is interesting to note that while Subjects 5 and 6 are the most consistent overall, they have completely opposite preferences. Subject 6 picks a winner according to the EMD ranking for 9 out of 12 evaluations, while Subject 5 is consistent with the OMCT ranking for 10 of the total 12 evaluations.

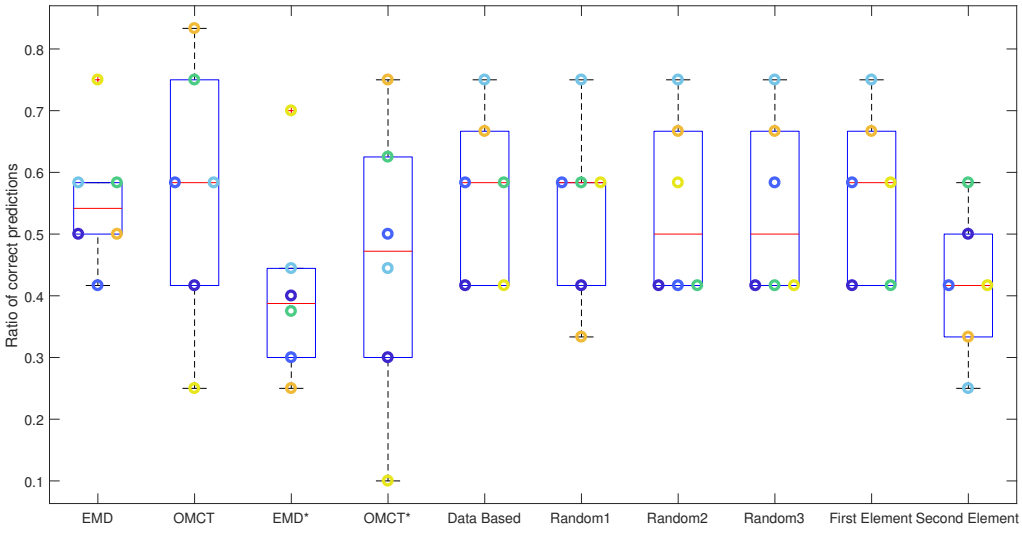

Fig. 10 Box plots of the ratio of correct predictions

By observing Fig. 10 it can be concluded that the main hypothesis is rejected as the medians of the complete and discriminatory OMCT ratios are higher than the medians of the corresponding EMD ratios. Furthermore, the difference between the two methods is not expected to be significant. This is confirmed with a statistical analysis. A non-parametric Friedmann ANOVA test is used for this, since the data does not satisfy the homogeneity of variance assumption. The results are $\chi^2(1) = 0.2, p = 0.65$ for both the complete ratios and the discriminatory pairs, indicating that for both of them the difference is indeed not significant.

Several other "predictors" are tested as well. They are not subjected to a statistical analysis, but serve as a baseline for the predictive performance of EMD. The first one is based on the ranking derived from the data with the Bradley-Terry model. Additionally, three random predictors are initialized with the following seeds:

1) The experiment date (e.g. *20180818*)
2) The subject number after the experiment date (e.g *201808183*)
3) The subject number before the experiment date (e.g *320180818*)

The random predictors are used as an unbiased measure to gauge the predictive capabilities of EMD and OMCT for pilot subjective cueing fidelity. It can clearly be seen in Fig. 10 that both methods do not seem to perform better than the random predictors. Finally, the ratio of wins for the first and second presented filter in the pair is compared in order to see if an order effect is present. Their corresponding box plots show a more noticeable difference in favour of the first element of the pair being preferred, which may potentially be significant. The result from the statistical test for the order effect is $\chi^2(3) = 0.964, p = 0.81$, meaning that it is not significant when taken over all pilots.

VI. Discussion

The main goal of this paper is to present the application of EMD to fixed-wing aircraft and investigate its capability to predict the subjective motion cueing fidelity perceived by pilots. In order to test this, six pilots compare four MCA configurations in pairs of two, by exciting the short period dynamics of a Cessna Citation 500 aircraft.

After completing the experiment all pilots reported they had difficulties in consistently giving evaluations of a high confidence, since according to them all four configurations had a similar feel. The test subjects gave a positive feedback on the pairwise comparison format of the experiment however, as it better enabled them to differentiate between the different configurations. Another opinion shared between the majority of the participants is that high frequency pitch oscillations, aiming to excite the short period dynamics for longer periods of time, were not beneficial for distinguishing

differences between the configurations. On the contrary, slower movements resulting from manoeuvres such as pitch angle intercepts enabled the pilots to better observe deficiencies in the motion. Therefore it is recommended that in future experiments a specifically defined task is used.

In addition, the pilot feedback indicates that the currently used EMD tuning approach can be improved upon by considering simultaneous tuning for the short period and phugoid. Since both eigenmodes are excited during longitudinal motions, a weighted tuning approach based on their relative MPFs for a set of manoeuvres can be investigated.

From the experiment results, it can be concluded that there are no significant differences between the predictive capabilities of EMD and OMCT. Both methods exhibit a performance similar to a random predictor, indicating that they are not the most reliable tools for predicting subjective cueing fidelity for MCA configurations which appear to be very similar, such as the ones used in this experiment.

Additionally, the accuracy of the ratios of correct predictions for EMD and OMCT can be argued, since some pilots tended to report varying levels of confidence when giving their evaluations. However, this was not done in a systematic manner for all pilots and was therefore not addressed in the statistical analysis. Should a similar experiment be attempted in future studies, it is recommended to add the confidence level of each evaluation to the dependent metrics. It can subsequently be used to improve the statistical modelling performed with the Bradley-Terry pattern model or another more complex method.

Furthermore, the subjective evaluation method of MCA configurations is not an inherently consistent and consequently reliable metric for measuring the predictive performance of EMD and OMCT. The evaluation criteria employed by different pilots can vary even when measures, such as providing universal instructions and briefing, are taken to minimize this. For instance, one pilot stated during the experiment that sometimes he might prefer a configuration that is not necessarily the most representative of the real aircraft, but more beneficial for training. Therefore it is recommended for future studies to investigate other more objective methods of quantifying and evaluating the performance of objective metrics such as EMD and OMCT.

Another observation based on the experiment results is that the currently used fidelity boundaries for OMCT need to be further refined, as there is a clearly expressed difference in the preference given to the two configurations conforming to OMCT, which is visible in the results for pair $B - O$. Studies have already been performed that analyze the fidelity boundaries based on pilot performance [1]. Similar research can be done with respect to different aircraft types and flight conditions.

Finally, the results of the pair $E_{ph} - E_m$ are unexpected, since these two conditions were hypothesized to be the most similar to one another and hence that pilots would find a little difference between them. The experiment showed that, on the contrary, this is the only pair where all pilots had consistent evaluations and on average E_{ph} is preferred to E_m. This is another indication for potential deficiencies in the currently used set of EMD based tuning criteria. Therefore further research into the methodology is needed.

VII. Conclusions

This paper presented the application of a novel method for objective motion cueing fidelity evaluation, Eigenmode Distortion, to fixed-wing aircraft. It was shown how this method can assess MCA settings for a specific aircraft model and flight condition, and how it can generate a ranking between MCA settings which sometimes conflicts with state-of-the-art OMCT assessments.

Validation through pilot opinion of both these ranking methods was hampered by inconsistencies between and within pilots. A reliable and objective "gold standard" to calibrate cueing assessment techniques that minimizes the influence of individual preferences and variability would strongly benefit a confident demonstration of EMD's value in the future. It is questionable if such a standard can (or should) be constructed without reference to expert pilot opinion.

In general EMD provides an alternative perspective on the tuning and assessment of motion cueing algorithms. It has the potential to identify issues with MCA configurations for a given flight condition that are not noticeable with the current objective criteria. Since the methodology is applicable to any aircraft throughout its flight envelope, it can be used as a stepping stone to understanding aircraft and flight condition specific motion cueing and for enhancing the currently used methods.

References

[1] Zaal, P. M. T., Schroeder, J. A., and Chung, W. W. Y., "Objective Motion Cueing Criteria Investigation Based on Three Flight Tasks," *Proceedings of the RAeS Flight Simulation Conference, 9-10 June 2015, London, UK*, Royal Aeronautical Society, 2015.

[2] Hosman, R. J. A. W., Advani, S. K., and Takats, J., "Status of the ICAO Objective Motion Cueing Test," *Autumn Flight Simulation Conference: Flight Simulation Research - New Frontiers*, Royal Aeronautical Society, Royal Aeronautical Society, 2012.

[3] Sinacori, J. B., "The Determination of Some Requirements for a Helicopter Research Simulation Facility," Tech. Rep. NASA-CR-152066, Systems Technology Inc., Sep. 1977.

[4] Schroeder, J. A., "Helicopter Flight Simulation Motion Platform Requirements," Tech. Rep. NASA-TP-1999-208766, National Aeronautics and Space Administration, Jul. 1999.

[5] Gouverneur, B., Mulder, J. A., van Paassen, M. M., Stroosma, O., and Field, E. J., "Optimisation of the SIMONA Research Simulator's Motion Filter Settings for Handling Qualities Experiments," *Proceedings of the AIAA Modeling and Simulation Technologies Conference and Exhibit, Austin, Texas, Aug. 11-14, 2003*, American Institute of Aeronautics and Astronautics, 2003.

[6] Hosman, R. J. A. W., "Are Criteria for Motion Cueing and Time Delays Possible?" *Proceedings of the AIAA Modelling and Simulation Technologies Conference and Exhibit, Portland (OR)*, American Institute of Aeronautics and Astronautics, 1999. doi:10.2514/6.1999-4028.

[7] Advani, S. K., and Hosman, R. J. A. W., "Revising Civil Simulator Standards – An Opportunity for Technological Pull," *Proceedings of the AIAA Modeling and Simulation Technologies Conference and Exhibit, Keystone (CO)*, American Institute of Aeronautics and Astronautics, 2006.

[8] Hosman, R. J. A. W., and Advani, S. K., "Are Criteria for Motion Cueing and Time Delays Possible? Part 2." *Proceedings of the AIAA Modeling and Simulation Technologies Conference, Boston (MA)*, American Institute of Aeronautics and Astronautics, 2013.

[9] Hosman, R. J. A. W., and Advani, S. K., "Design and Evaluation of the Objective Motion Cueing Test and Criterion," *The Aeronautical Journal*, Vol. 120, No. 1227, 2016, pp. 873–891. doi:10.1017/aer.2016.35.

[10] Anonymous, "Manual of Criteria for the Qualification of Flight Simulation Training Devices. Volume 1 – Airplanes," ICAO Doc 9625, International Civil Aviation Organization, 2015. Fourth edition.

[11] De Ridder, K., and Roza, M., "Automatic Optimization of Motion Drive Algorithms using OMCT," *AIAA Modeling and Simulation Technologies Conference, Kissimmee, FL*, American Institute of Aeronautics and Astronautics, 2015, p. 1139.

[12] Dalmeijer, W., Miletović, I., Stroosma, O., and Pavel, M. D., *Extending the Objective Motion Cueing Test to Measure Rotorcraft Simulator Motion Characteristics*, 2017, pp. 1876–1891.

[13] Miletović, I., Pavel, M. D., Stroosma, O., Pool, D. M., van Paassen, M. M., Wentink, M., and Mulder, M., "Motion Cueing Fidelity in Flight Simulation: A Novel Perspective," 2018. To be submitted.

[14] Reid, L. D., and Nahon, M. A., "Flight Simulation Motion-Base Drive Algorithms. Part 1: Developing and Testing the Equations," Tech. Rep. UTIAS 296, University of Toronto, Institute for Aerospace Studies, Dec. 1985.

[15] Stroosma, O., van Paassen, M. M., and Mulder, M., "Using the SIMONA Research Simulator for Human-machine Interaction Research," *Proceedings of the AIAA Modeling and Simulation Technologies Conference and Exhibit, Austin, Texas, Aug. 11-14, 2003*, American Institute of Aeronautics and Astronautics, 2003, pp. 1–8.

[16] Seehof, C., Durak, U., and Duda, H., "Objective Motion Cueing Test - Experiences of a New User," *AIAA Modeling and Simulation Technologies Conference, Atlanta, Georgia, US*, , No. AIAA 2014-2205, 2014, pp. 1–14. doi:10.2514/6.2014-2205.

[17] Oppenheim, A. V., and Verghese, G. C., *Signals, systems and inference*, 1st ed., Pearson, Hoboken, NJ, 2015, Chap. 5.

[18] Stroosma, O., van Paassen, M. M., Mulder, M., Hosman, R. J. A. W., and Advani, S. K., "Applying the Objective Motion Cueing Test to a Classical Washout Algorithm," *Proceedings of the AIAA Modeling and Simulation Technologies Conference, Boston (MA)*, American Institute of Aeronautics and Astronautics, 2013.

[19] Zaichik, L. E., Yashin, Y. P., and Desyatnik, P., "Peculiarities of Motion Cueing for Precision Control Tasks and Maneuvers," *ICAS. Nice, France. ICAS Paper*, Vol. 602, 2010.

[20] Cattelan, M., "Models for Paired Comparison Data: A Review with Emphasis on Dependent Data," *Statistical Science*, 2012, pp. 412–433.

[21] Hatzinger, R., and Dittrich, R., "Prefmod: An R Package for Modelling Preferences Based on Paired Comparisons, Rankings, or Ratings," *Journal of Statistical Software*, Vol. 48, No. 10, 2012, pp. 1–31.